A Tristable Mechanism Configuration Employing Orthogonal Compliant Mechanisms

Guimin Chen[1]
School of Mechatronics,
Xidian University,
Xi'an, Shaanxi 710071, China
e-mail: guimin.chen@gmail.com

Quentin T. Aten
e-mail: quentinaten@yahoo.com

Shannon Zirbel
e-mail: sazirbel@gmail.com

Brian D. Jensen
e-mail: bdjensen@byu.edu

Larry L. Howell
e-mail: lhowell@byu.edu

Department of Mechanical Engineering,
Brigham Young University,
Provo, UT 84602

Tristable mechanisms, or devices with three distinct stable equilibrium positions, have promise for future applications, but the complexities of the tristable behavior have made it difficult to identify configurations that can achieve tristable behavior while meeting practical stress and fabrication constraints. This paper describes a new tristable configuration that employs orthogonally oriented compliant mechanisms that result in tristable mechanics that are readily visualized. The functional principles are described and design models are derived. Feasibility is conclusively demonstrated by the successful operation of four embodiments covering a range of size regimes, materials, and fabrication processes. Tested devices include an in-plane tristable macroscale mechanism, a tristable lamina emergent mechanism, a tristable micromechanism made using a carbon nanotube-based fabrication process, and a polycrystalline silicon micromechanism.
[DOI: 10.1115/1.4000529]

1 Introduction

Tristable mechanisms have three stable equilibrium positions within their range of motion. In these equilibrium positions, the mechanism can maintain stability without power input. Tristable mechanisms may be useful in many applications, such as switches, valves, transistors, mechanical memory, multiplex optical switches, and positioners, to name a few. Although there are many potential applications, the complexities of creating tristable behavior have resulted in few configurations that are capable of tristable behavior within practical limits on stress. This is particularly true when fabrication constraints require that the device be constructed of one piece and any motion results in elastic energy being stored in flexible elements. Compliant mechanisms, which achieve at least some of their mobility from the deflection of flexible segments rather than from movable joints only, offer a possible way to achieve tristable behavior [1]. Deriving configurations of tristable mechanisms is nontrivial because of the competing requirements to create multiple stable equilibrium positions. Balancing the competing forces often causes high stresses that are infeasible for practical implementation.

The literature contains many examples of bistable mechanisms [2–10], including methods for synthesis of new bistable mechanisms [11,12]. Multistable mechanisms with more than two stable equilibrium positions have received less attention, although a few examples exist. For example, Pendleton and Jensen [13,14] presented a partially compliant tristable mechanism based on a four-bar model and a wire-form tristable mechanism, Chen et al. [15] presented a new class of tristable mechanisms called double tensural tristable mechanisms (DTTMs), which incorporate flexible elements experiencing combined tension and bending, and Oberhammer et al. [16] demonstrated a tristable mechanism that depends on friction and latching to achieve its three positions. Multistable mechanisms have also been demonstrated by combining together two or more bistable mechanisms to achieve four or more stable states [17–19]. Ohsaki and Nisiwaki [20] also demonstrated multistable mechanisms using pin-jointed elements in a snap-through arrangement, and King et al. [21,22] developed optimization techniques for the design of multistable compliant mechanisms.

Tristable mechanisms offer challenges in creating devices that can provide the proper force balancing of different energy storage components to create the desired positions. This force balancing is particularly difficult when done under the stress constraints of the flexible members. Fully compliant mechanisms offer unique challenges because the energy storage elements are flexible members under stress, and although the fundamental mechanics show it is theoretically possible to create fully compliant tristable mechanisms, the practical stress limits make most configurations infeasible for operation. These stress constraints are particularly challenging for micromechanical devices where the fabrication processes limit the geometries and materials that can be employed. This has led to the criticism that while theoretical tristable devices are available, the state of knowledge has not yet expanded to generate tristable mechanisms that can meet the practical limitations of stress and fabrication constraints. This paper addresses that criticism by expanding the body of knowledge in tristable mechanisms as follows: (i) a general tristable mechanism configuration is identified that has straightforward mechanics, where the tristable behavior is readily identified; (ii) an approach for designing these mechanisms is illustrated; and (iii) device feasibility is definitively demonstrated by the successful operation of four physical instantiations of designs that cover a wide range of sizes, materials, and fabrication processes.

2 Tristable Mechanism Configuration

The new tristable mechanism configurations proposed in this paper employ orthogonal compliant mechanisms to achieve three stable equilibrium positions. Figure 1 demonstrates one possible configuration of this kind of tristable mechanism. In this design, the end-effector travels in the positive and negative y-directions, and the bistable mechanism, which displaces in the positive x-direction, provides the force required to deflect the end-effector to a stable equilibrium position. A schematic of the tristable mechanism in its three stable equilibrium positions is shown in Fig. 2. One benefit of this configuration is that the mechanics causing the tristable behavior are readily apparent. However, there are still significant challenges to achieve the proper function given practical constraints of stress and manufacturing limits. This is particularly true for micromechanisms, where brittle materials are often required because of the fabrication processes used. The end-

[1]Corresponding author. Present address: P. O. Box 181, No. 2 Taibai South Road, Xi'an, Shaanxi 710071, China.
Contributed by the Mechanisms and Robotics Committee of ASME for publication in the JOURNAL OF MECHANISMS AND ROBOTICS. Manuscript received July 17, 2009; final manuscript received September 26, 2009; published online November 19, 2009. Editor: J. Michael McCarthy.

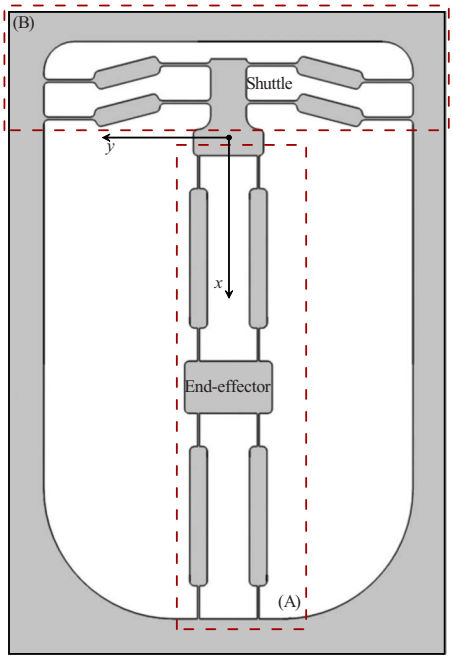

Fig. 1 A design example (device A): (*a*) end-effector; (*b*) bistable mechanism

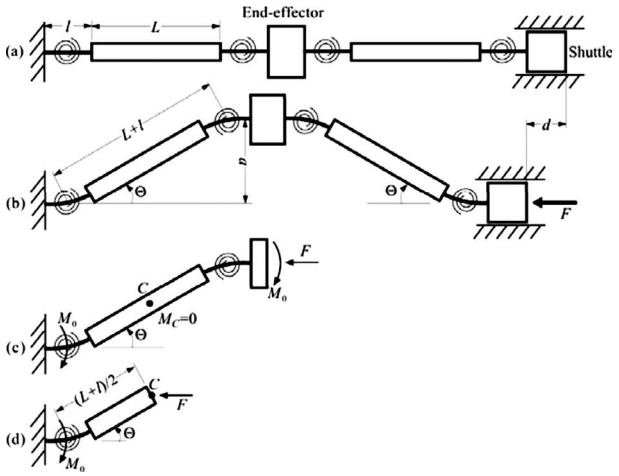

Fig. 3 (*a*) As-fabricated position, (*b*) deformed position, and (*c*) free-body diagram of one-half and (*d*) one-quarter of the end-effector

effector portion must have adequate motion and have low enough forces to not overcome the force available from the bistable portion, while the bistable portion must provide enough latching force to contain its own elastic energy and the return energy from the end-effector. In Sec. 3, the design considerations which can be used to ensure device tristability are discussed.

3 Tristable Behavior and Design

This section discusses the design issues that guarantee tristability of the proposed mechanism configuration.

Figure 3 shows a single linkage of the pseudo-rigid-body model (PRBM) of the end-effector, and gives the free-body diagram for both one-half and one-quarter of the end-effector. The PRBM treats one-half of the end-effector as a fixed-guided segment and the flexible members as small-length flexural pivots [1].

The displacement d of the shuttle along the x-axis is approximated (note that the length of the pseudo-rigid-body link is $L+l/2+l/2=L+l$) as

$$d = 2(L + l)(1 - \cos \Theta) \tag{1}$$

and the displacement of the end-effector along the y-axis is approximated as

$$a = (L + l)\sin \Theta \tag{2}$$

where Θ is the corresponding pseudo-rigid-body angle.

Because the deformed shape of one-half of the model is antisymmetric, the moment at the center point C is zero, i.e., $M_C=0$. Thus, the force required to deflect the shuttle to position d can be calculated as

$$F = \frac{2N_p K\Theta}{(L + l)\sin \Theta} \tag{3}$$

where N_p is the number of flexible segment sets in parallel (e.g., $N_p=2$ in Fig. 1), $\Theta \neq 0$ (but note that $\Theta/\sin \Theta$ approaches 1 as Θ approaches 0), and K is the torsional stiffness of the small-length flexural pivots, which can be expressed as

$$K = \frac{EI}{l} \tag{4}$$

where E is the Young's modulus of the material, and I and l are the moment of inertia and the length of the small-length flexural pivots, respectively.

By substituting Eq. (1) into Eq. (3), the force-deflection (F to d) relationship of the end-effector is given by

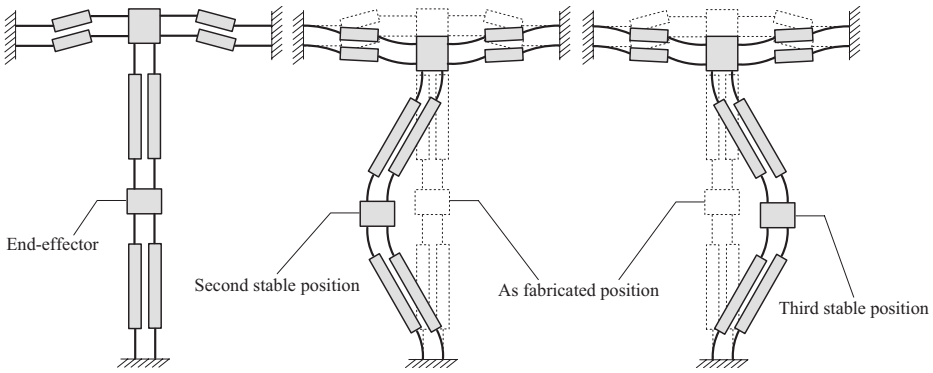

Fig. 2 A tristable mechanism illustrated in its three stable equilibrium positions, including its as-fabricated (left), second stable (middle), and third stable (right) positions

Table 1 Design parameterss (see Figs. 3 and 5)

	Parameter	Device A	Device B	Device C	Device D
End-effector	E	2.4×10^9 Pa	2.4×10^9 Pa	1.2×10^{11} Pa	1.65×10^{11} Pa
	L	41.5 mm	43.6 mm	88 μm	50 μm
	l	9 mm	9.5 mm	100 μm	180 μm
	h	6.2 mm	10 mm	25 μm	3.5 μm
	w	0.5 mm	0.75 mm	1.5 μm	3 μm
	N_p	2	1	2	1
Bistable mechanism	H	6.2 mm	12.4 mm	25 μm	3.5 μm
	L_1	14 mm	14 mm	57.3 μm	57.3 μm
	θ_1	0 deg	0 deg	6.6 deg	6.6 deg
	w_1	1 mm	1 mm	3 μm	3 μm
	L_2	9 mm	9.5 mm	126.3 μm	126.3 μm
	θ_2	14 deg	14 deg	5.6 deg	5.6 deg
	w_2	5.2 mm	5.2 mm	8 μm	8 μm
	L_3	14 mm	14 mm	75.7 μm	75.7 μm
	θ_3	0 deg	0 deg	6.4 deg	6.4 deg
	w_3	1 mm	1 mm	3 μm	3 μm

$$F = \frac{4N_pK \arccos\left[1 - \dfrac{d}{2(L+l)}\right]}{\sqrt{4(L+l)d - d^2}} \tag{5}$$

By using Eq. (5), the force-deflection characteristics of the end-effector of device A (the corresponding parameters are given in Table 1) in Fig. 1 is achieved. The change in force is small over the range of the input deflection. Figure 4 compares the force-deflection characteristics of the end-effector (shown as a dashed line) with the output-force-deflection characteristics of the bistable mechanism (the solid curve), which is achieved using nonlinear finite element analysis. F_C is the maximum output force and F_S is the force required to switch the device past its unstable equilibrium point [8]. For a design to exhibit multistability, F_C must be larger than the force needed to hold the end-effector at position "C." If this condition is satisfied, then there is an intersection point of the bistable mechanism and end-effector force-deflection curves. This intersection, labeled as position "B" in Fig. 4, is a stable equilibrium position. Because the geometry is symmetric, there is another stable equilibrium position when the end-effector moves in the opposite direction. These two positions plus the as-fabricated position result in three stable equilibrium positions and the device is tristable.

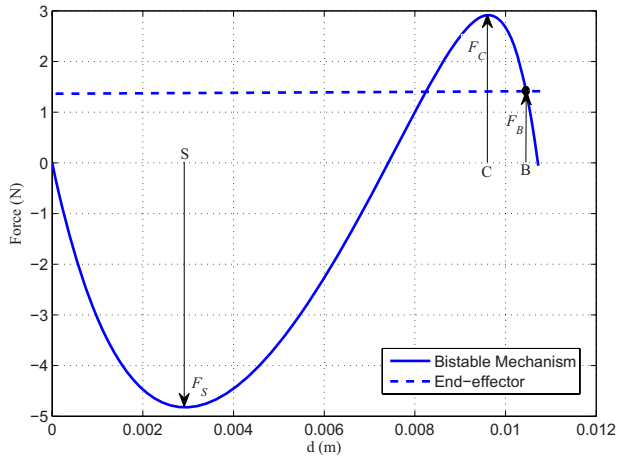

Fig. 4 Force-deflection curves of device A

4 Demonstration Devices

The feasibility of this fully compliant tristable mechanism configuration was conclusively demonstrated by the physical prototype devices. Four designs were selected to represent a wide range of sizes, materials, and fabrication methods. The first two devices are macroscale devices and were machined from polypropylene. These two devices were selected because the first mechanism (device A) has an end-effector motion within the plane of fabrication, while the other device (device B) has an end-effector motion out of the plane of fabrication (and thus it is a lamina emergent mechanism [23]) and results in different loads on the bistable portion. Devices C and D are microscale devices and are fabricated from different materials using different processes. These demonstrate device feasibility in environments highly constrained by fabrication and material limitations.

Figures 3 and 5 and Table 1 give the design parameters of the devices. The out-of-plane thickness of the end-effector is h and the width of the flexible segments is w. The in-plane parameters of the bistable mechanism portion of the microdevices are similar to those in Ref. [24] and are the results of extensive research in bistable micromechanisms. The constraints on the macrodevices allow L_1 and L_3 to be symmetric, thus simplifying their design. The values for E for devices A, B, and D are based on extensive laboratory experience with the materials and are consistent with published ranges. Device C is constructed from a new material and the reported value of E is an estimate based on preliminary work [25].

4.1 Device A. Device A, as shown in Fig. 6, is a macroscale planar tristable mechanism fabricated from polypropylene. Figure 6(*a*) shows the first stable equilibrium, or as-fabricated position. The second stable equilibrium position is shown in Fig. 6(*b*). Figure 6(*c*) shows the third stable equilibrium position. As expected, the second and third positions are symmetric about the first positions. The model successfully predicted the tristable behavior and

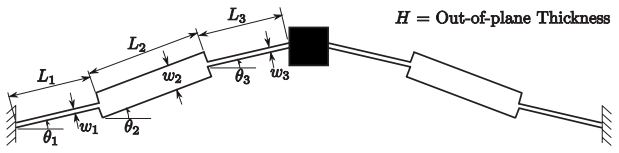

Fig. 5 Dimensions of bistable mechanism employed in the test devices

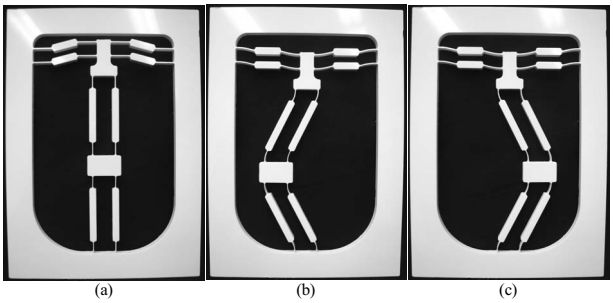

Fig. 6 Planar tristable mechanism: (*a*) fabricated, or first, (*b*) second, and (*c*) third stable equilibrium positions

made a reasonable prediction for the location of the stable equilibrium positions. The predicted (as shown in Fig. 4) and measured values for the stable equilibrium positions are listed in Table 2. The deflections were measured using calipers.

4.2 Device B. Figure 7 shows device B, which is a lamina emergent tristable mechanism fabricated from polypropylene. Lamina emergent mechanisms are compliant mechanisms manufactured from sheet goods with motion out of the plane of manufacture [23]. The lamina emergent tristable mechanism, providing two stable equilibrium positions out of the plane of manufacture, was tested and demonstrated to have tristable behavior, as shown in Figs. 7(*b*) and 7(*c*). Figure 8 compares the force-deflection characteristics of the lamina emergent mechanisms (LEM) end-effector (dashed line) with the output-force-deflection characteristics of the bistable mechanism (solid curve). The predicted and measured values for the stable equilibrium positions are listed in Table 3, as measured using calipers.

4.3 Device C. To demonstrate applicability in the microregime, a planar tristable micromechanism (device C) was fabricated using a process that uses carbon nanotubes (CNTs) in a silicon matrix [26,25]. The mechanism was fabricated by patterning an alumina diffusion layer and an iron seed layer in the desired shape of the tristable mechanism. A carbon nanotube "forest" was then grown in a furnace to a height of about 25 μm. Polycrystalline silicon was deposited in a low-pressure chemical vapor deposition (LPCVD) process. The LPCVD silicon coated

Table 2 The predicted and measured values (±0.1 mm) for the stable equilibrium positions of device A

	Predicted d	Measured d	Predicted a	Measured a
1st stable position	0	0	0	0
2nd stable position	10.5 mm	10.1 mm	22.4 mm	22.8 mm
3rd stable position	10.5 mm	10.2 mm	−22.4 mm	−22.9 mm

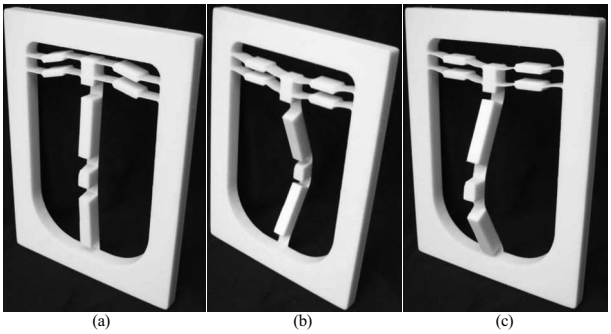

Fig. 7 Lamina emergent tristable mechanism: (a) fabricated, or first, (b) second, and (*c*) third stable equilibrium positions

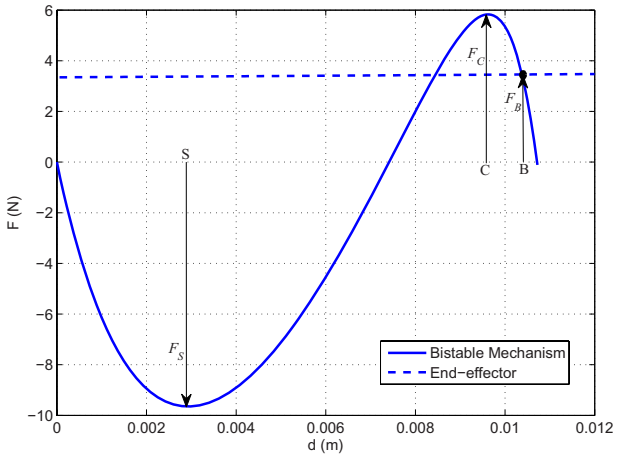

Fig. 8 Force-deflection curves of device B

the nanotubes and joined them together into a solid composite material. Finally, the moveable parts of the mechanism were released by dissolving the underlying layers using wet chemical etchants. The result is a free-standing MEMS structure with high out-of-plane thickness (about 25 μm) compared with in-plane width (a minimum of 1.5 μm). Other work has proposed using CNTs as flexible segments in nanocompliant mechanisms [27], but the present work differs in that it uses many CNTs in a composite material to create a micro mechanism. A picture of a device using an optical microscope is shown in Fig. 9. Two of the three stable positions are illustrated, with the third being symmetric with the second position, as described in other devices. The residue in the image is debris from the release process.

4.4 Device D. A tristable mechanism was fabricated using a surface micromachining process and polycrystalline silicon (PolyMUMPs [28]). Figure 10 shows the SEM images of a tristable device in its second and third stable equilibrium positions, with its as-fabricated state taken with an optical microscope shown as an inset. The nominal dimensions of the micromechanism are listed in Table 3. A scanning electron microscope was used to measure

Table 3 The predicted and measured values (± 0.1 mm) for the stable equilibrium positions of device B (note that *a* is along the *z*-axis for device B)

	Predicted d	Measured d	Predicted a	Measured a
1st stable position	0	0	0	0
2nd stable position	10.5 mm	10.2 mm	23.0 mm	23.5 mm
3rd stable position	10.5 mm	10.2 mm	−23.0 mm	−23.4 mm

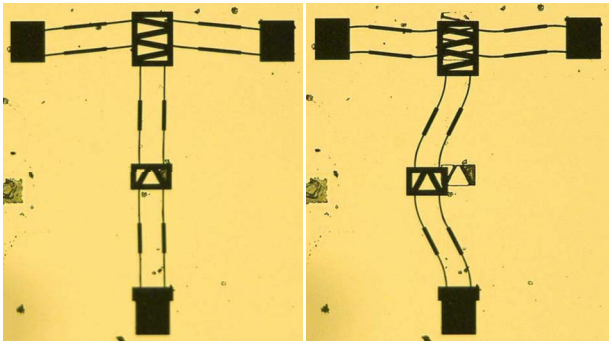

Fig. 9 A tristable micromechanism made using a carbon nanotube-based fabrication process

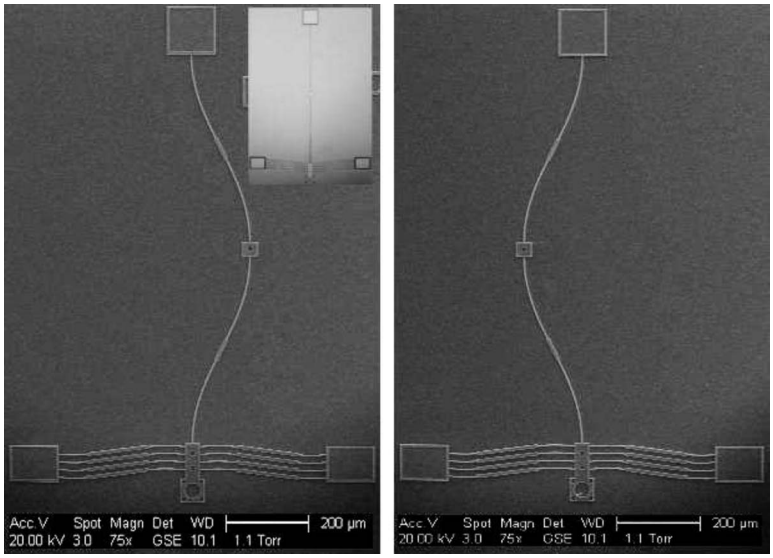

Fig. 10 Scanning electron micrographs of the tristable micromechanism fabricated from polycrystalline silicon. The inset optical image shows the device in its undeflected state and the other two images demonstrate the second and third stable equilibrium positions.

the width of the 3 μm legs, showing that the final leg width was 2.87 μm. The end-effector stiffness resulted in forces that tended to cause the bistable mechanism to have motion out of the plane. This parasitic motion has been observed in similar mechanisms [24]. The motion can be reduced by physical constraints, such as using a higher layer of polysilicon to cap the shuttle out-of-plane motion, or microprobes which used in this testing.

5 Conclusion

This paper has described a new tristable mechanism configuration and has demonstrated its feasibility via four different physical instantiations, representing designs covering a range of size regimes, fabrication processes, and materials. Models were developed for device design and the results compared favorably with model predictions. The paper results are intended to facilitate device implementation by providing a straightforward description of the device mechanics, demonstrating an approach for device design, and showing feasibility in various situations.

All the designs demonstrated in this paper are symmetric. Nevertheless, selecting nonsymmetric designs can result in nonsymmetric placement of equilibrium positions. This nonsymmetry can be achieved by causing the direction of motion of the end-effector to be nonorthogonal to the bistable mechanism's motion. The force characteristics would also be affected; each direction could be tailored to specific force-deflection characteristics, which may benefit some applications. The bistable mechanisms incorporated into the tristable mechanisms above can be replaced by any kind of bistable mechanism that provides linear motion, such as those found in Refs. [7,8].

Acknowledgment

The authors gratefully acknowledge the financial support from the U.S. National Science Foundation under Grant No. CMMI-0800606, the National Natural Science Foundation of China under Grant No. 50805110, the Key Project of Chinese Ministry of Education under Grant No. 109145, and the China Postdoctoral Science Foundation under Grant No. 20070421110. The assistance of David Hutchison, Nathan Morrill, and the staff of the Integrated Microfabrication Laboratory of Brigham Young University in fabrication of device C is also gratefully acknowledged. Guimin Chen was a visiting scholar in the Compliant Mechanisms Research Group at Brigham Young University in Oct. 2007–Oct. 2008.

References

[1] Howell, L., 2001, *Compliant Mechanisms*, Wiley, New York.
[2] Hälg, B., 1990, "On a Micro-Electro-Mechanical Nonvolatile Memory Cell," IEEE Trans. Electron Devices, **37**(10), pp. 2230–2236.
[3] Hwang, I.-H., Shim, Y.-S., and Lee, J.-H., 2003, "Modeling and Experimental Characterization of the Chevron-Type Bi-Stable Microactuator," J. Micromech. Microeng., **13**(6), pp. 948–954.
[4] Qiu, J., Lang, J., and Slocum, A., 2004, "A Curved-Beam Bistable Mechanism," J. Microelectromech. Syst., **13**(2), pp. 137–146.
[5] Charlot, B., Sun, W., Yamashita, K., Fujita, H., and Toshiyoshi, H., 2008, "Bistable Nanowire for Micromechanical Memory," J. Micromech. Microeng., **18**(4), p. 045005.
[6] Kwon, H.-N., Hwang, I.-H., and Lee, J.-H., 2005, "A Pulse-Operating Electrostatic Microactuator for Bi-Stable Latching," J. Micromech. Microeng., **15**(8), pp. 1511–1516.
[7] Masters, N., and Howell, L., 2003, "A Self-Retracting Fully Compliant Bistable Micromechanism," J. Microelectromech. Syst., **12**(3), pp. 273–280.
[8] Wilcox, D., and Howell, L., 2005, "Double-Tensural Bistable Mechanisms (DTBM) With On-Chip Actuation and Spring-Like Post-Bistable Behavior," ASME Paper No. DETC2005-84697.
[9] Wilcox, D. L., and Howell, L. L., 2005, "Fully Compliant Tensural Bistable Micromechanisms (FTBM)," J. Microelectromech. Syst., **14**, pp. 1223–1235.
[10] Sönmez, U., and Tutum, C., 2008, "A Compliant Bistable Mechanism Design Incorporating Elastica Buckling Beam Theory and Pseudo-Rigid-Body Model," ASME J. Mech. Des., **130**(4), p. 042304.
[11] Jensen, B., and Howell, L., 2003, "Identification of Compliant Pseudo-Rigid-Body Four-Link Mechanism Configurations Resulting in Bistable Behavior," ASME J. Mech. Des., **125**(4), pp. 701–708.
[12] Jensen, B., and Howell, L., 2004, "Bistable Configurations of Compliant Mechanisms Modeled Using Four Links and Translational Joints," ASME J. Mech. Des., **126**(4), pp. 657–666.
[13] Pendleton, T., and Jensen, B., 2007, "Development of a Tristable Compliant Mechanism," *Proceedings of the 12th IFToMM World Congress*, Paper No. A835.
[14] Pendleton, T., and Jensen, B., 2008, "Compliant Wireform Mechanisms," ASME J. Mech. Des., **130**(12), p. 122302.
[15] Chen, G., Wilcox, D., and Howell, L., 2009, "Fully Compliant Double Tensural Tristable Micromechanisms (DTTM)," J. Micromech. Microeng., **19**(2), p. 025011.
[16] Oberhammer, J., Tang, M., Liu, A., and Stemme, G., 2006, "Mechanically Tri-Stable, True Single-Pole-Double-Throw (SPDT) Switches," J. Micromech. Microeng., **16**(11), pp. 2251–2258.
[17] Han, J., Muller, C., Wallrabe, U., and Korvink, J., 2007, "Design, Simulation, and Fabrication of a Quadstable Monolithic Mechanism With X- and Y-Directional Bistable Curved Beams," ASME J. Mech. Des., **129**(11), pp. 1198–1203.
[18] Oh, Y., and Kota, S., 2009, "Synthesis of Multi-Stable Equilibrium Compliant

Mechanisms Using Combinations of Bistable Mechanisms," ASME J. Mech. Des., **131**, p. 021002.
[19] Gerson, Y., Krylov, S., Ilic, B., and Schreiber, D., 2008, "Large Displacement Low Voltage Multistable Micro Actuator," *Proceedings of the IEEE 21st International Conference on Micro Electro Mechanical Systems*, pp. 463–466.
[20] Ohsaki, M., and Nishiwaki, S., 2005, "Shape Design of Pin-Jointed Multistable Compliant Mechanisms Using Snapthrough Behavior," Struct. Multidiscip. Optim., **30**(4), pp. 327–334.
[21] King, C., Beaman, J., Sreenivasan, S., and Campbell, M., 2004, "Multistable Equilibrium System Design Methodology and Demonstration," ASME J. Mech. Des., **126**(6), pp. 1036–1046.
[22] King, C., Campbell, M., Beaman, J., and Sreenivasan, S., 2005, "Synthesis of Multistable Equilibrium Linkage Systems Using an Optimization Approach," Struct. Multidiscip. Optim., **29**(6), pp. 477–487.
[23] Jacobsen, J., Winder, B., Howell, L., and Magleby, S., 2010, "Lamina Emergent Mechanisms and Their Basic Elements," ASME J. Mech. Rob., **2**, p. 011003.
[24] Cherry, B., Howell, L., and Jensen, B., 2008, "Evaluating Three-Dimensional Effects on the Behavior of Compliant Bistable Micromechanisms," J. Micromech. Microeng., **18**(9), p. 095001.
[25] Hutchison, D., Aten, Q., Turner, B., Morrill, N., Howell, L., Jensen, B., Davis, R., and Vanfleet, R., 2009, "High Aspect Ratio Microelectromechanical Systems: A Versatile Approach Using Carbon Nanotubes as a Framework," *Proceedings of the Transducers 2009*.
[26] Hayamizu, Y., Yamada, T., Mizuno, K., Davis, R., Futaba, D., Yumura, M., and Hata, K., 2008, "Integrated Three-Dimensional Microelectromechanical Devices From Processable Carbon Nanotube Wafers," Nat. Nanotechnol., **3**(5), pp. 289–294.
[27] DiBiasio, C., Culpepper, M., Panas, R., Howell, L., and Magleby, S., 2008, "Comparison of Molecular Simulation and Pseudo-Rigid-Body Model Predictions for a Carbon Nanotube-Based Compliant Parallel-Guiding Mechanism," ASME J. Mech. Des., **130**(4), p. 042308.
[28] 2005, "Polymumps Design Handbook," www.memsrus.com/documents/PolyMUMPs.DR.v11. pdf